NÖHÜ Müh. Bilim. Derg. / NOHU J. Eng. Sci., 16 (2026), 1773776
Niğde Ömer Halisdemir Üniversitesi Mühendislik Bilimleri Dergisi
Niğde Ömer Halisdemir University Journal of Engineering Sciences
Araştırma makalesi / Research article
www.dergipark.org.tr/tr/pub/ngumuh / www.dergipark.org.tr/en/pub/ngumuh

Biosynthesis of CdS nanoparticles using mushroom (*Macrolepiota procera*) extracts and characterization

Mantar (*Macrolepiota procera*) özütleri kullanılarak CdS nanopartiküllerinin biyosentezi ve karakterizasyonu

Ali Zeytünlüoğlu[1], Osman Çaylak[2], Halil İbrahim Çetintaş[3,*]

[1]*Pamukkale University, Denizli Vocational School of Technical Sciences, Department of Chemistry and Chemical Processing Technologies, 20160, Denizli, Türkiye*
[2]*Sivas Cumhuriyet University, Vocational School of Health Services, Department of Pharmacy, 58140, Sivas, Türkiye*
[3]*Sivas Cumhuriyet University, Faculty of Engineering, 58140, Sivas, Türkiye*

Abstract

In this study, cadmium sulfide (CdS) nanoparticles were synthesized using crude extract of *Macrolepiota procera* (MP) as a biogenic reducing and stabilizing agent. The synthesized nanoparticles were characterized for their morphological structure, elemental composition, crystal structure, functional group content, and optical bandgap properties using FE-SEM, EDX, XRD, FTIR, and UV-Vis spectroscopy. FE-SEM images revealed that the nanoparticles exhibited a predominantly spherical morphology. EDX analysis indicated that the atomic ratio of Cd to S was approximately 1:1, confirming the stoichiometry of CdS. XRD results showed that CdS nanoparticles synthesized with MP-10 exhibited a cubic crystalline phase, with theoretical particle sizes estimated to be between 2.44 and 2.90 nm. FTIR analysis confirmed the presence of phytochemicals from the MP extract on the nanoparticle surface, acting as capping and stabilizing agents, consistent with previous reports. UV-Vis spectroscopy demonstrated that the bandgap energies of CdS-MP5, CdS-MP7.5, and CdS-MP10 were 2.65, 2.77, and 2.87 eV, respectively, all higher than that of bulk CdS (2.42 eV), indicating quantum confinement effects.

Keywords: Green synthesis, Mushroom, *Macrolepiota procera*, CdS nanoparticles

Öz

Bu çalışmada, kadmiyum sülfür (CdS) nanoparçacıkları, *Macrolepiota procera* (MP) ham ekstraktı biyojenik bir indirgeme ve stabilizasyon ajanı olarak kullanılarak sentezlenmiştir. Sentezlenen nanoparçacıklar; morfolojik yapıları, elementel bileşimleri, kristal yapıları, fonksiyonel grup içerikleri ve optik bant aralığı özellikleri açısından FE-SEM, EDX, XRD, FTIR ve UV-Vis spektroskopisi kullanılarak karakterize edilmiştir. FE-SEM görüntüleri, nanoparçacıkların ağırlıklı olarak küresel bir morfoloji sergilediğini ortaya koymuştur. EDX analizi, Cd ile S arasındaki atomik oranın yaklaşık 1:1 olduğunu göstermiş ve CdS'nin stokiyometrisini doğrulamıştır. XRD sonuçları, MP-10 kullanılarak sentezlenen CdS nanoparçacıklarının kübik kristal faza sahip olduğunu ve teorik parçacık boyutlarının 2.44 ile 2.90 nm arasında değiştiğini göstermiştir. FTIR analizi, MP ekstraktından kaynaklanan fitokimyasalların nanoparçacık yüzeyinde bulunduğunu ve bu bileşiklerin kaplayıcı ve stabilize edici ajanlar olarak görev yaptığını, önceki çalışmalarla uyumlu şekilde doğrulamıştır. UV–Vis spektroskopisi, CdS-MP5, CdS-MP7.5 ve CdS-MP10 örneklerinin bant aralığı enerjilerinin sırasıyla 2.65, 2.77 ve 2.87 eV olduğunu göstermiştir. Bu değerler, yığın CdS'nin bant aralığı enerjisinden (2.42 eV) daha yüksek olup, boyuta bağlı kuantum sınırlanma etkilerinin varlığına işaret etmektedir.

Anahtar kelimeler: Yeşil sentez, Mantar, *Macrolepiota procera*, CdS nanopartiküller

1 Introduction

In recent years, nanomaterials have garnered substantial attention across a broad spectrum of scientific and technological disciplines—including medicine, environmental science, cosmetics, automotive engineering, food technology, energy systems, and electronics—owing to their distinctive chemical, magnetic, optical, electrical, and electronic characteristics. Conventionally, these nanostructures have been synthesized through a variety of physicochemical techniques, including hydrothermal reactions, microwave-assisted synthesis, solvothermal procedures, and chemical reduction methods. Despite their widespread utility, these approaches frequently require toxic reducing or capping agents, such as thioacetamide and mercaptoethanol, which introduce significant environmental and human health concerns. Additionally, conventional synthesis routes often involve extended reaction times, elevated temperatures, and specialized instrumentation, thereby constraining their operational feasibility and long-term sustainability [1, 2].

To mitigate these limitations, green synthesis strategies have emerged as a compelling and environmentally benign alternative to traditional physicochemical methods. These

* Sorumlu yazar / Corresponding author, e-posta / e-mail: hcetintas@cumhuriyet.edu.tr (H. İ. Çeliktaş)
Geliş / Received: 02.09.2025 Kabul / Accepted: 22.01.2026 Yayımlanma / Published: 05.02.2026
doi: 10.28948/ngumuh.1773776

sustainable approaches exploit the intrinsic reducing and stabilizing capacities of various biological systems—including plants, microorganisms, algae, and fungi thus eliminating the necessity for hazardous chemicals and energy-intensive conditions [3]. Among these biological platforms, fungi have attracted particular scientific interest as highly efficient biofactories for metal nanoparticle synthesis. Their metabolic repertoire, comprising diversified extracellular enzymes, reductase systems, proteins, polysaccharides, and additional bioactive metabolites, enables the simultaneous bioreduction of metal ions and stabilization of nanoparticle surfaces. The natural biomolecular coatings impart enhanced colloidal stability, morphological uniformity, and functional surface chemistry. Moreover, the capacity of fungi to mediate both intracellular and extracellular nanoparticle formation facilitates scalability, promotes controlled biosynthesis, and simplifies downstream purification. Collectively, fungal-based nanomaterial synthesis constitutes a sustainable, cost-effective, and high-efficiency strategy with broad implications for environmental remediation, biomedical innovation, energy conversion, and advanced materials engineering.

A growing body of literature has underscored the diverse biological functionalities of fungus-derived nanoparticles. Owaid demonstrated that silver nanoparticles synthesized using *Pleurotus ostreatus* exhibit robust antibacterial, antifungal, anticancer, and antioxidant activities [4]. Similarly, Chaturvedi reported pronounced anticancer efficacy of silver and gold nanoparticles biosynthesized from *Pleurotus sajor-caju* polysaccharides [5]. Investigations on *Ganoderma lucidum* have revealed that AgNPs derived from this species possess strong antimicrobial activity against both Gram-positive and Gram-negative bacterial strains [6], while gold nanoparticles synthesized from *G. lucidum* exert substantial anticancer effects on HT-29 colon cancer cells [7]. Additional reports include marked antibacterial efficacy of AgNPs synthesized from *Agaricus bisporus* [8], the anticancer potential of a *Amanita muscaria*-based silver nanoparticle–hyaluronic acid gel formulation [9], and the growth-promoting activity of MgO nanoparticles on peanut seedlings [10]. Selenium nanoparticles derived from *Hymenopellis radicata* polysaccharides have been shown to exhibit superior antioxidant activity [11], whereas FeONPs synthesized using *Pleurotus citrinopileatus* demonstrate antibacterial and anticancer properties [12]. TiO_2 nanoparticles sourced from *Hypsizygus ulmarius* have similarly displayed anticancer activity against HepG2 liver cancer cells and inhibited several human pathogens [13]. Furthermore, ZnO nanoparticles synthesized using *Trichoderma harzianum* effectively suppressed *Alternaria brassicae* even at low concentrations [14], and those derived from the endophyte *Xylaria acuta* exhibited broad-spectrum antibacterial and anticancer activities [15]. Collectively, these findings underscore the extensive versatility and biomedical significance of fungal and other biologically derived nanoparticles.

Parallel to these advancements, cadmium sulfide (CdS) nanoparticles have emerged as a central focus of contemporary nanotechnology research owing to their tunable optical and electronic properties, predominantly governed by size-dependent quantum confinement effects. Nanoscale modulation of bandgap energy, enhancement of photoluminescence quantum yield, and controlled tuning of light absorption across the visible spectrum render CdS nanoparticles highly advantageous for diverse applications, including photocatalytic water splitting, visible-light-driven degradation of organic pollutants, high-sensitivity sensing platforms, and optoelectronic device engineering [16]. Additionally, their intrinsically high specific surface area, elevated surface reactivity, and chemically tailorable surface architecture support their integration into hybrid composites and fluorescent nanoprobes for biomedical imaging. Consequently, research on precisely controlled CdS nanoparticle synthesis remains essential for driving innovations in next-generation environmental, biomedical, and energy-related technologies.

In this context, CdS nanoparticles have been increasingly utilized across a broad spectrum of medical, environmental, and food-related fields. Reported applications encompass drug-delivery [16], biosensing technologies [17], bioimaging modalities [18–21], antimicrobial activity [22–24], cancer therapy [25–27], antifungal activity [28], photocatalysis [29, 30], photooxidation processes [31], photoreduction reactions [32, 33], biofilm-based food packaging systems [34], and optoelectronic device fabrication [35, 36].

The biological synthesis and functional activities of CdS nanoparticles have been the subject of extensive investigation. Elhenawy reported that CdS nanoparticles synthesized using *Agaricus bisporus* extract effectively inhibited the development of *Musca domestica* larvae, a vector associated with more than one hundred infectious pathogens [37]. Veeramani demonstrated that zinc-doped CdS nanoparticles (Zn–CdS NPs) synthesized using *Hypsizygus ulmarius* mitigated Paclobutrazol-induced toxicity in *Danio rerio* embryos and larvae [38]. Plant-mediated synthesis approaches have also yielded promising outcomes; for instance, Faisal observed considerable antibacterial and antifungal activity of CdS nanoparticles produced using *Lathyrus aphaca* [39], whereas Jameel documented potent insecticidal, antibacterial, and anticancer effects of CdS nanoparticles synthesized from Nopal cactus fruit extract [40]. CdS nanoparticles derived from *Camellia sinensis* leaves exhibited antibacterial activity, cytotoxicity toward A549 lung cancer cells, and pronounced fluorescence for bioimaging applications [20]. Additional studies have demonstrated the antimicrobial and anticancer potential of CdS nanoparticles synthesized using *Aspergillus niger* [41] and the pro-apoptotic activity of CdS quantum dots derived from *Raphanus sativus* roots against MCF-7 breast cancer cells [42]. Collectively, these findings reflect the considerable biological versatility of CdS nanoparticles synthesized via fungi, plants, bacteria, and yeasts.

Beyond their biological functionalities, substantial efforts have also been directed toward optimizing CdS synthesis protocols, characterizing structural and optical properties, and evaluating environmental applications. For

example, Tudu provided comprehensive physicochemical characterization of CdS nanoparticles synthesized using *Termitomyces heimii* extract [43]. Pandian synthesized CdS nanoparticles using *Brevibacterium casei* SRKP2 and subsequently encapsulated the nanoparticles within polyhydroxybutyrate (PHB) matrices [44]. Sanghi and Verma emphasized the critical role of fungal thiol groups in CdS formation using immobilized *Coriolus versicolor* [45]. Lakshmipathy synthesized CdS nanoparticles through a one-step green synthesis method using agricultural waste, specifically watermelon rind [46] while Elakkiya further demonstrated the capacity of watermelon rind–derived CdS nanoparticles to remove Methylene Blue and Crystal Violet dyes from aqueous systems [47]. Additional studies include CdS biosynthesis by *Lactobacillus* sp. and *Saccharomyces cerevisiae* [48], size-controlled CdS formation using immobilized *Rhodobacter sphaeroides* [49], and the production of CdS quantum dots via *Pleurotus ostreatus* mycelium [50].

Macrolepiota procera, an edible parasol mushroom belonging to the class Agaricomycetes (Figure 1), represents a particularly promising macrofungal candidate for the biosynthesis of metal nanoparticles.

Figure 1. Morphological structure of *M. procera*

Its rapid growth rate and high biomass-generating capacity, combined with a metabolome enriched in phenolic compounds, flavonoids, proteins, polysaccharides, and various oxidoreductase systems, collectively facilitate efficient metal ion bioreduction and nanoparticle stabilization. These biomolecular constituents act synergistically as natural reducing and capping agents, promoting enhanced control over nanoparticle morphology and enabling the synthesis of nanostructures with improved uniformity. Accordingly, the biochemical versatility and metabolic richness of *M. procera* render it a valuable organism for sustainable, environmentally benign, and scalable nanoparticle production [51–55].

In the present study, CdS nanoparticles were synthesized via a biogenic approach employing *Macrolepiota procera* extract as an economical, ecologically sustainable, and environmentally benign green synthesis agent. The synthesized nanoparticles were subjected to detailed morphological, structural, elemental, and optical characterization to elucidate their physicochemical attributes.

2 Materials and methods

2.1 Collection of mushroom samples

M. procera mushroom was collected from a rural area in the Acıpayam District of Denizli, Turkey. The mushroom bodies were thoroughly washed with distilled water for removal of the soil and other residues from the mushroom surface. After washing, the mushrooms were air-dried.

2.2 Preparation of mushroom extract

Dried mushroom samples were ground into powder using a grinder. Ten grams of powdered mushroom samples were added to a beaker containing 150 mL of deionized water and maintained at constant stirring at 80 °C for 1 hour. The solution was cooled to room temperature and centrifuged at 3,000 rpm for 10 minutes, and the supernatant was separated and stored at 4°C for further analysis.

2.3 Synthesis of CdS nanoparticles

50 mL of $Cd(NO_3)_2$ solution was mixed with different volumes of mushroom extract: 5 mL, 7.5 mL, and 10 mL, corresponding to the samples MP-5, MP-7.5, and MP-10, respectively. 0.1 M Na_2S was added dropwise to the mixture. The solution was stirred at 60-80ºC in the dark for 16 hours. The reaction was terminated when the color of the solution changed from brown to orange. The solution was centrifuged at 10,000 rpm for 10 minutes at room temperature. The resulting pellet was washed twice with distilled water, followed by centrifugation after each washing step. Then the pellet was dried (Figure 2).

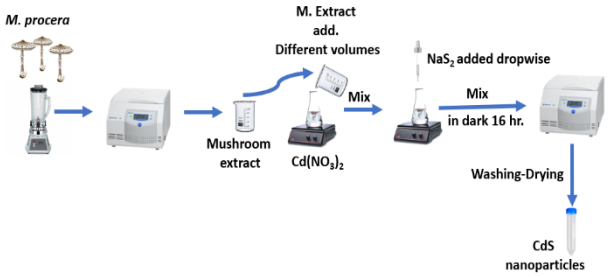

Figure 2. Schematic representation for CdS nanoparticle synthesis using *M. procera* extract

2.4 Characterization of CdS nanoparticles

The synthesized materials were thoroughly characterized using various analytical techniques, including UV-Vis (ultraviolet-visible spectroscopy), FTIR (Fourier transform infrared spectroscopy), XRD (X-ray diffraction), FE-SEM (field emission scanning electron microscopy), and EDX (energy dispersive X-ray spectroscopy) analyses.

2.4.1 UV–Vis analysis

CdS nanoparticles synthesized using *M. procera* were dispersed in DMSO using an ultrasonic bath and immediately transferred into a 10 mm quartz cuvette. UV-Vis spectra were then recorded without delay using a Lambda 20 UV/VIS spectrophotometer (PerkinElmer, Varian, Australia), scanning in the range of 400–800 nm.

2.4.2 FTIR analysis

The screening of functional groups on the surface of the CdS nanoparticles in the mid-infrared region (400–4000 cm^{-1}) was performed using FTIR spectrometer (Bruker Tensor II, United States) equipped with a diamond crystal

ATR (Attenuated Total Reflectance) accessory, with a spectral resolution of 4 cm^{-1} and 16 scans.

2.4.3 XRD analysis

XRD analysis was performed to investigate the crystallinity of the CdS-MP10 nanoparticles, which were selected for this analysis because they exhibited the smallest particle size according to UV-Vis spectroscopy results. The diffraction patterns were recorded in the 2θ range of 10° to 80° using an XRD (Malvern Panalytical, United Kingdom) equipped with Cu Kα radiation (λ = 1.5406 Å) at a scan rate of 1°/min.

2.4.4 FE-SEM and EDX analysis

The morphological properties, particle size, and elemental composition of CdS-MP10 nanoparticles were examined using FE-SEM and EDX analysis (Tescan Mira3 XMU, Czech Republic). The nanoparticle powder was dispersed onto carbon tapes and analyzed without coating, as the samples were conductive.

3 Results and discussion

3.1 UV–Vis analysis

UV-Vis absorption spectroscopy, which is a cost-effective, easily accessible, and rapid technique, is known to be an effective technique for quantitative determinations as well as for monitoring the optical properties of nanomaterials, which are directly related to particle size. CdS powder synthesized using the M. procera mushroom extract was dispersed in a 10 mm quartz cuvette using an ultrasonic bath in DMSO, and the spectra were demonstrated in the range of 400-800 nm (Figure 3). The maximum absorptions were found at 468, 448, and 432 nm for CdS-MP5, CdS-MP7.5, and CdS-MP10, respectively.

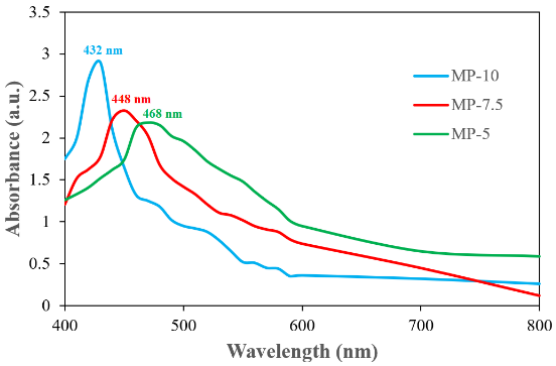

Figure 3. UV–Vis spectra of the synthesized CdS samples

The spectra clearly show a significant blue shift in the UV–vis absorption edge of the green-synthesized CdS nanoparticles compared to bulk CdS (λbulk=515 nm, Eg(bulk)=2.42 eV. This blueshift tendency arises directly from the quantum confinement effect, resulting from the reduced particle size and the consequent widening of the band gap [56, 57]. The energy band gap of the green synthesized CdS nanoparticles was estimated using Equation (1) [58].

$$E_g(eV) = \frac{hc}{\lambda_{max}(nm)} = \frac{1242}{\lambda_{max}(nm)} \quad (1)$$

Here, *Eg* is the energy bandgap (eV), *c* is the velocity of light (2.998×108 ms-1), *h* is Planck's constant (6.626×10-34 Js), and *λmax* is the wavelength at which maximum absorption occurs. The estimated values of band gap energy for CdS-MP5, CdS-MP7.5 and CdS-MP10 are 2.65, 2.77 and 2.87 eV, respectively. These values were high compared to the bulk CdS band gap of 2.42 eV. This clearly demonstrates the nanoscale nature of the CdS nanoparticles and their size-dependent optical behavior. As the particle diameter gradually decreases, the energy levels become increasingly separated. Consequently, a reduction in the particle size of the synthesized nanoparticles with increasing fungal concentration was associated with an increase in the band gap [59].

The wavelength of maximum absorption (λ_{max}), which is commonly used in the literature for an initial evaluation of quantum confinement effects and particle size trends, was used in this study to estimate the optical band gap energies. It is crucial to remember that the onset wavelength (λ_{onset}) obtained from the absorption edge should be used for a more accurate measurement of the optical band gap because it directly relates to the fundamental electronic transition [60]. Future in-depth optical investigations should use the λ_{onset} method for improved accuracy in absolute band gap quantification, even though the λ_{max}-based values presented here provide a consistent comparative trend across our samples and match observable blue shifts.

Using the energy ranges obtained from the synthesized CdS nanoparticles, the particle size of the quantum dots was obtained by the Brus equation, one of the widely used theoretical models (Equation (2)) [61].

$$E_g(nano) - E_g(bulk) = \frac{h^2}{2D^2}\left(\frac{1}{m_e^*} + \frac{1}{m_h^*}\right) - \frac{3.6e^2}{4\pi\varepsilon D} \quad (2)$$

Here, E_g(nano) and E_g(bulk) (2.42 eV) denote the bandgaps of CdS nanoparticles and bulk CdS, respectively. m_e^* (0.19 m_e) and m_h^* (0.8 m_e) represent the effective masses of electrons and holes, respectively. ε is the dielectric constant ($5.7\varepsilon_0$), where ε_0 is the permittivity of free space (8.85×10^{-12} $C^2 N^{-1} m^{-2}$). *r* is the radius of CdS nanoparticles, *h* is Planck's constant, and *e* is the elementary charge (1.6×10^{-19} C).

The diameters of the green synthesized CdS nanoparticles were estimated using the empirical equations found by Yu et al. (Equation (3)) and Henglein (Equation (4)) in addition to the Brus equation [62, 63].

$$D = -6.65x10^{-8}\lambda^3 + 1.96x10^{-4}\lambda^2 - 9.24x10^{-2}\lambda + 13.29 \quad (3)$$

$$D = \frac{0.1}{0.1338 - 0{,}0002345\lambda} \quad (4)$$

In these empirical equations, λ represents the wavelength of the absorption peak (λ_max) of the CdS nanoparticles in

nanometers (nm), as used in the cited references [64, 65]. The particle sizes of CdS nanoparticles calculated using equations 2, 3, and 4 were presented in Table 1. The size of fungal synthesized CdS nanoparticles was generally small compared to bulk CdS crystals (5.6 nm). It is estimated that this is due to the stabilizing effect of fungal proteins that act as capping agents [2, 45].

Table 1. Spectroscopic parameters and particle sizes calculated from UV-Vis spectra of synthesized CdS nanoparticles

Sample	λ_{max} (nm)	Eg (eV)	Particle size (nm)		
			Brus	Yu	Henglein
CdS (MP-5)	468	2.65	4.83	6.16	4.16
CdS (MP-7.5)	448	2.77	4.15	5.25	3.48
CdS (MP-10)	432	2.87	3.76	4.59	3.08

The effect of the amount of *M. procera* biomass extract on the sizes of CdS nanoparticles calculated from empirical formulas is given in Figure 4**.** It is clearly seen from the figure that the nanoparticle size decreases as the amount of extract used in the synthesis increases. This indicates that the CdS nanoparticle size can be adjusted by the amount of *M. procera* extract. The results obtained are compatible with the literature [43, 50, 66].

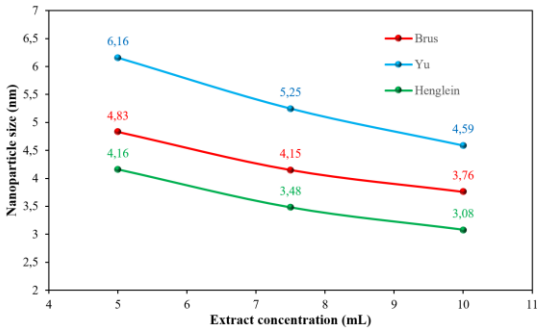

Figure 4. Effect of MP concentration on the size of CdS nanoparticles

3.2 FTIR analysis

Fourier transform infrared spectroscopy (FTIR) is one of the most common analytical methods used to characterize the structure of both organic and inorganic materials. This technique, which provides detailed information about the chemical properties of materials, is also frequently used in the analysis of metallic nanoparticles [67]. FTIR is also successfully employed to identify the functional groups and phytoconstituents present on the surface of the nanoparticles [68]. In this context, the FTIR spectra of CdS nanoparticles using MP extract at various concentrations are shown in Figure 5.

Since CdS synthesis was carried out with the same procedure for all extract concentrations, the FTIR spectra of the nanoparticles appeared almost the same except for the differences in the intensity of the peaks, related to the amount of functional groups on the nanoparticle surface. A broad absorption band observed around 3200 cm^{-1} is attributed to the O–H and N–H stretching vibrations of hydroxyl and amine groups. These functional groups originate from phenolic compounds, alcohols, and proteins present in the mushroom extract. The weak bands appearing at ~2350 cm^{-1} are commonly associated with the asymmetric stretching vibration of atmospheric CO_2 due to the environmental artefacts rather than the sample. The absorption band at 2113 cm^{-1} may be attributed to weak C≡C or C≡N stretching vibrations, which can arise from minor organic constituents or secondary metabolites present in the mushroom extract. The broad band between 1900–1700 cm^{-1} may be attributed to overtone or combination vibrations related to carbonyl (C=O) groups, possibly associated with proteinaceous components or amide functionalities. The major peaks of the protein structure are observed at 1627 cm^{-1} and 1553 cm^{-1} due to the amide I and amide II bands, respectively. Another characteristic peak of the mushroom proteins related to the C-H bending vibrations is observed at 1405 cm^{-1}. In addition, C-O stretching vibrations, thought to belong to alcohol, ether or ester groups, appeared as a series of consecutive peaks between 1100 cm^{-1} and 1000 cm^{-1}. The main bands belong to Cd-S stretching vibrations, which indicate CdS nanoparticle formation, were observed at 604 and 527 cm^{-1}, in agreement with the literature studies [69, 70]. FTIR results show that functional structures in biomolecules found in mushroom extracts play a important role in CdS nanoparticle synthesis and stabilization as stated in the literature [29, 44].

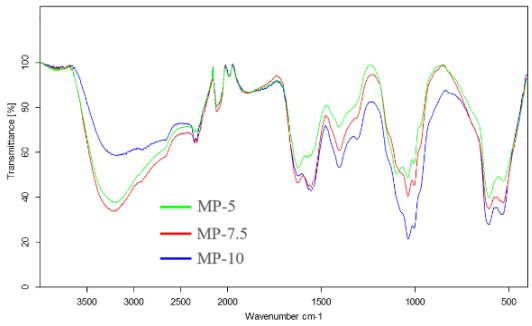

Figure 5. FTIR spectra of CdS samples

3.3 XRD analysis

XRD, which is one of the most preferred powerful techniques in determining variables such as crystal structure, crystal phase and lattice parameters of synthesized nanoparticles, was used for the characterization of the CdS nanoparticles we synthesized. Figure 6 shows the XRD pattern of the crystallinity of green synthesized CdS nanoparticles. According to the results we obtained from the empirical formulas used, MP-10, which had the smallest particle size, was preferred for the XRD spectrum. In Figure 6, there exist tetra peaks at 26.70◦, 44.05◦, 52.00 and 71.20◦, which correspond to (111), (220), (311) and (331) planes in cubic phase of CdS according to ICDD (89-0440) [71].

The X-ray diffraction profiles clearly show that the intensity of the (111) reflection is significantly higher than that of the other diffraction peaks, indicating a preferred orientation. This confirms that the nanoparticles exhibit a face-centered cubic (FCC) crystal structure [72, 73]. No additional peaks corresponding to secondary phases or

impurities were observed, confirming the high phase purity of the CdS nanoparticles. Furthermore, while XRD reveals the internal crystal geometry of the nanoparticles, FTIR analysis confirms the presence of surface-bound biomolecules, indicating successful stabilization without altering the crystalline framework. The obtained lattice parameters are compatible with literature data [74–76]. Crystallite sizes were calculated using the Dybe Scherrer expression given in Equation (5) [77].

$$D_{average}(\text{average crystallite size}) = \frac{K\lambda}{\beta cos\theta} \quad (5)$$

Where, K is the Debye–Scherer constant (0.94, 'K' value varying between 0.8 and 1.2 (typically equal to 0.9)), λ is the wavelength of CuKα radiation (0.154 nm), β is the full width at half maximum (FWHM in radians) of the peak, θ is the Bragg angle (Peak position (radians)). From the Scherer equation, the sizes of the particles were calculated in the range of 2.44 to 2.90 nm (Table 2).

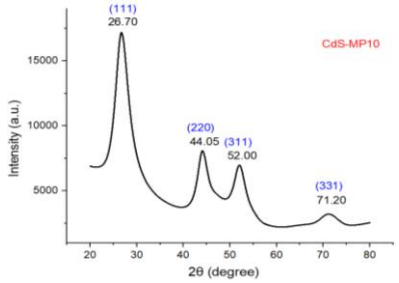

Figure 6. Powder XRD patterns of CdS samples

3.4 FE-SEM and EDX analysis

Field Emission Scanning Electron Microscopy (FE-SEM) is a potent technique that has recently become widely used for high-resolution imaging of materials and determining the dimensional and morphological properties at both the micro and nanoscales. In the characterization of nanoparticles, FE-SEM enables obtaining both physical and chemical information, especially when used in conjunction with other powerful analysis techniques such as energy-dispersive X-ray spectroscopy (EDX). Due to the smallest size, morphological and elemental characterization of CdS-MP10 nanoparticles was conducted using FE-SEM and EDX analysis, and the results are given in Figure 7.

According to the FE-SEM image given in Figure 7(a), CdS nanoparticles were successfully synthesized through the biogenic method using MP mushroom extract. The nanoparticles were spherical in shape and agglomerated. This agglomeration was thought to be gravitational agglomeration due to the small particle size [78]. In addition, it is known that changing surface properties due to dense functional groups added to their structures may affect the agglomeration behavior of nanoparticles [79]. Thus, nanoparticles can appear larger than they actually are. Also according to the EDX analysis results shown in Figure 7(b), atomic percentages of Cd and S elements were quite close. This proves that the obtained chemical structure is in the form of CdS compound. In addition, the fact that Cd and S elements are found in the same regions in EDX mapping analyzes confirms the CdS structure (Figure 7(c)). It is thought that the intense amounts of C and O elements originate from the functional groups and phytochemicals on the nanoparticle surface, which is in good agreement with the FTIR results confirming surface-bound organic moieties.

4 Conclusion

The role of mushrooms in human life has been increasing due to advances in mushroom cultivation techniques. In parallel, there has been a growing interest in utilizing mushrooms beyond their traditional role as a food source, particularly owing to their rich metabolite content. One promising application is the biogenic synthesis of nanoparticles, which offers environmentally friendly and cost-effective advantages. Nanoparticles synthesized through this green method are being widely investigated for their potential use in medical, agricultural, and environmental applications.

In this study, CdS nanoparticles were synthesized via biogenic methods using *M. procera* mushroom extracts highlighting the eco-friendly and economical nature of the process. Characterization studies confirmed the successful and desirable size properties of the synthesized CdS nanoparticles. FE-SEM analysis revealed spherical morphology, while EDX results indicated a Cd:S atomic ratio of approximately 1:1, consistent with the stoichiometry of CdS. XRD analysis demonstrated that the nanoparticles exhibited a cubic crystalline phase, with theoretical particle sizes ranging between 2.44 and 2.90 nm. FT-IR spectra confirmed the presence of phytochemicals on the nanoparticle surface, acting as stabilizing and capping agents. UV-Vis spectroscopy showed that the band gap energies of the CdS nanoparticles were higher than that of bulk CdS, indicating size-dependent quantum confinement effects. These findings demonstrate the potential of MP extract as a sustainable and effective biogenic medium for producing CdS nanoparticles with controlled size and enhanced optical features. In future work, it may be possible to purify the specific metabolites responsible for nanoparticle synthesis or produce them recombinantly in large quantities to enhance nanoparticle production. Furthermore, key parameters such as yield, particle size, and morphology can be optimized based on the intended application area.

Table 2. XRD parameters of CdS nanoparticles (MP10 sample)

Sample	2θ/degree	θ/degree	Miller Indices	FWHM (°)	β (radian)	Size (nm)
MP10	26.70	13.35	111	3.493	0.0610	2.44
	44.05	22.03	220	3.160	0.0552	2.83
	52.00	26.00	311	3.180	0.0555	2.90
	71.20	35.60	331	4.080	0.0712	2.50

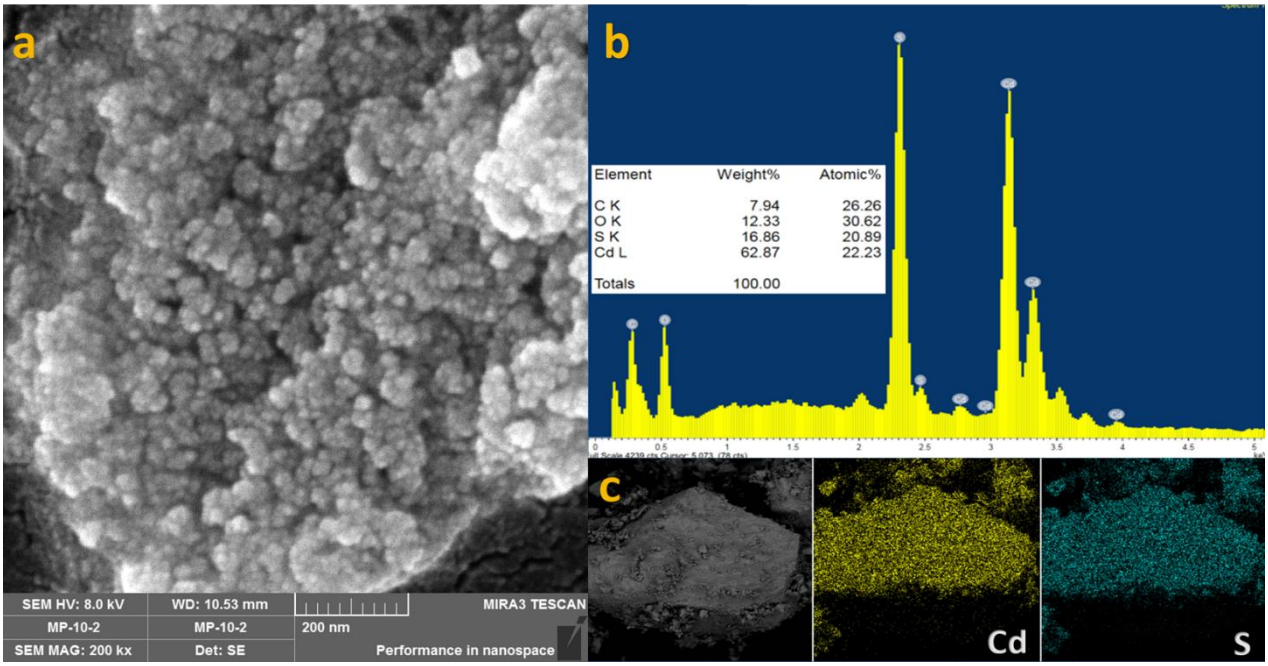

Figure 7. (a) FE-SEM image of nanoparticles, (b) EDX spectra and quantitative analysis results, (c) EDX mapping of CdS-MP10.

Conflict of interest

The authors declare that there is no conflict of interest.

Similarity rate (iThenticate): %20

References

[1] H. Dabhane, S. Ghotekar, P. Tambade, S. Pansambal, H. A. Murthy, R. Oza, V. Medhane, A review on environmentally benevolent synthesis of CdS nanoparticle and their applications, Environmental chemistry and ecotoxicology, 3, 209–219, 2021. https://doi.org/10.1016/j.enceco.2021.06.002

[2] M. D. Rao and G. Pennathur, Green synthesis and characterization of cadmium sulphide nanoparticles from Chlamydomonas reinhardtii and their application as photocatalysts, Materials Research Bulletin, 85, 64–73, 2017. https://doi.org/10.1016/j.materresbull.2016.08.049

[3] H. İ. Çetintaş, Biogenic Synthesis and Characterization of Silver Nanoparticles Using Hoya Carnosa Flower Extract, Cumhuriyet Science Journal, 46, (2), 286–291, 2025. https://doi.org/10.17776/csj.1607025

[4] M. N. Owaid, Green synthesis of silver nanoparticles by Pleurotus (oyster mushroom) and their bioactivity: Review, Environmental Nanotechnology, Monitoring and Management, 12:100256, 2019. https://doi.org/10.1016/j.enmm.2019.100256

[5] V. K. Chaturvedi, N. Yadav, N. K. Rai, N. H. A. Ellah, R. A. Bohara, I.F. Rehan, N. Marraiki, G. E. S. Batiha, H. F. Hetta, M. P. Singh, *Pleurotus sajor-caju*-Mediated Synthesis of Silver and Gold Nanoparticles Active against Colon Cancer Cell Lines: A New Era of Herbonanoceutics. Molecules, *25*(13), 2020. https://doi.org/10.3390/molecules25133091

[6] M. Constantin, I. Răut, R. Suica-Bunghez, C. Firinca, N. Radu, A. M. Gurban, S. Preda, E. Alexandrescu, M. Doni, L. Jecu, *Ganoderma lucidum*-Mediated Green Synthesis of Silver Nanoparticles with Antimicrobial Activity. Materials, 16(12), 2023. https://doi.org/10.3390/ma16124261

[7] D. Elumalai, T. Y. Suman, M. Hemavathi, C. Swetha, R. Kavitha, C. Arulvasu, P. K. Kaleena, Biofabrication of gold nanoparticles using *Ganoderma lucidum* and their cytotoxicity against human colon cancer cell line (HT-29). Bulletin of Materials Science, 44, 132, 2021. https://doi.org/10.1007/s12034-021-02435-0

[8] M. Amr, S. H. Abu-Hussien, R. Ismail, A. Aboubakr, R. Wael, M. Yasser, B. Hemdan, S. M. El-Sayed, A. Bakry, N. M. Ebeed, H. Elhariry, A. Galal, B. T. Abd-Elhalim, Utilization of biosynthesized silver nanoparticles from *Agaricus bisporus* extract for food safety application: synthesis, characterization, antimicrobial efficacy, and toxicological assessment. Scientific Reports, 13, 15048, 2023. https://doi.org/10.1038/s41598-023-42103-3

[9] O. Ivashchenko, Ł. Przysiecka, B. Peplińska, M. Jarek, E. Coy, S. Jurga, Gel with silver and ultrasmall iron oxide nanoparticles produced with *Amanita muscaria* extract: physicochemical characterization, microstructure analysis and anticancer properties. Scientific Reports, 8, 13260, 2018. https://doi.org/10.1038/s41598-018-31686-x

[10] K. Jhansi, N. Jayarambabu, K. P. Reddy, N. M. Reddy, R. P. Suvarna, K. V. Rao, V. R. Kumar, V. Rajendar, Biosynthesis of MgO nanoparticles using mushroom extract: effect on peanut (*Arachis hypogaea* L.) seed germination. 3 Biotech, 7, 263, 2017. https://doi.org/10.1007/s13205-017-0894-3

[11] Y. Liu, W. Huang, W. Han, C. Li, Z. Zhang, B. Hu, S. Chen, P. Cui, S. Luo, Z. Tang, W. Wu, Q. Luo, Structure characterization of *Oudemansiella radicata* polysaccharide and preparation of selenium nanoparticles to enhance the antioxidant activities. LWT - Food Science and Technology, 146, 2021. https://doi.org/10.1016/j.lwt.2021.111469

[12] K. Manimaran, D. H. Y. Yanto, M. Govindasamy, B. Karunanithi, F.A. Alasmary, R. A. Habab, Biological synthesis and characterization of iron oxide (FeO) nanoparticles using *Pleurotus citrinopileatus* extract and its biomedical applications. Biomass Conversion and Biorefinery, 14, 12575–12585, 2024. https://doi.org/10.1007/s13399-023-04382-8

[13] K. Manimaran, S. Loganathan, D. G. Prakash, D. Natarajan, Antibacterial and anticancer potential of mycosynthesized titanium dioxide (TiO_2) nanoparticles using *Hypsizygus ulmarius*. Biomass Conversion and Biorefinery, 1–9, 2022. https://doi.org/10.1007/s13399-022-03186-6

[14] D. N. Mishra, L. Prasad, U. Suyal, Synthesis of zinc oxide nanoparticles using *Trichoderma harzianum* and its bio-efficacy on *Alternaria brassicae*. Frontiers in Microbiology, 16, 1506695, 2025. https://doi.org/10.3389/fmicb.2025.1506695

[15] B. Sumanth, T. R. Lakshmeesha, M. A. Ansari, M. A. Alzohairy, A. C. Udayashankar, B. Shobha, S. R. Niranjana, C. Srinivas, A. Almatroudi, Mycogenic synthesis of extracellular zinc oxide nanoparticles from *Xylaria acuta* and its nanoantibiotic potential. International Journal of Nanomedicine, 15, 8519–8536, 2020. https://doi.org/10.2147/IJN.S271743

[16] A. Ghasempour, H. Dehghan, M. Ataee, B. Chen, Z. Zhao, M. Sedighi, X. Guo, M.-A. Shahbazi, Cadmium sulfide nanoparticles: preparation, characterization, and biomedical applications. Molecules, 28(9), 3857, 2023. https://doi.org/10.3390/molecules28093857

[17] V. Pardo-Yissar, E. Katz, J. Wasserman, I. Willner, Acetylcholine esterase-labeled CdS nanoparticles on electrodes: photoelectrochemical sensing of the enzyme inhibitors. Journal of the American Chemical Society, 125(3), 622–623, 2003. https://doi.org/10.1021/ja028922k.

[18] R. Harish, K. D. Nisha, S. Prabakaran, B. Sridevi, S. Harish, M. Navaneethan, S. Ponnusamy, Y. Hayakawa, C. Vinniee, M. R. Ganesh, Cytotoxicity assessment of chitosan-coated CdS nanoparticles for bio-imaging applications. Applied Surface Science, 499, 143817, 2020. https://doi.org/10.1016/j.apsusc.2019.143817

[19] N. Órdenes-Aenishanslins, G. Anziani-Ostuni, J. P. Monrás, A. Tello, D. Bravo, D. Toro-Ascuy, R. Soto-Rifo, P. N. Prasad, J. M. Pérez-Donoso, Bacterial synthesis of ternary CdSAg quantum dots through cation exchange: tuning the composition and properties of biological nanoparticles for bioimaging and photovoltaic applications. Microorganisms, 8(5), 631, 2020. https://doi.org/10.3390/microorganisms8050631

[20] K. Shivaji, S. Mani, P. Ponmurugan, C. S. De Castro, M. L. Davies, M. G. Balasubramanian, S. Pitchaimuthu, Green-Synthesis-Derived CdS Quantum Dots Using Tea Leaf Extract: Antimicrobial, Bioimaging, and Therapeutic Applications in Lung Cancer Cells, ACS Applied Nano Materials, 1(4), 1683–1693, 2018. https://doi.org/10.1021/acsanm.8b00147

[21] Q. Wu, L. Huang, Z. Li, W. An, D. Liu, J. Lin, L. Tian, X. Wang, B. Liu, W. Qi, W. Wu, The Potential Application of Raw Cadmium Sulfide Nanoparticles as CT Photographic Developer, Nanoscale Research Letters, 11, (1), 232, 2016. https://doi.org/10.1186/s11671-016-1424-7

[22] A. Calvo-Olvera, M. De Donato-Capote, H. Pool, N. G. Rojas-Avelizapa, In vitro toxicity assessment of fungal-synthesized cadmium sulfide quantum dots using bacteria and seed germination models, Journal of Environmental Science and Health, Part A, 56, (6), 713–722, 2021. https://doi.org/10.1080/10934529.2021.1899718

[23] A. León-Buitimea, C. R. Garza-Cárdenas, J. A. Garza-Cervantes, J. A. Lerma-Escalera, J. R. Morones-Ramírez, The demand for new antibiotics: antimicrobial peptides, nanoparticles, and combinatorial therapies as future strategies in antibacterial agent design, Frontiers in microbiology, 11, 1669, 2020. https://doi.org/10.3389/fmicb.2020.01669

[24] P. V. Sekar, V. D. Parvathi, R. Sumitha, Green nanotechnology in cadmium sulphide nanoparticles and understanding its toxicity and antimicrobial properties, Biomed. Res, 30(5), 805, 2019. https://doi.org/10.35841/biomedicalresearch.30-19-324

[25] T. Nasrin, M. Patra, S. M. Rahaman, T. K. Das, S. Shaikh, Biosynthesized CdS Nanoparticle Induces ROS-dependent Apoptosis in Human LungCancer Cells, Anti-Cancer Agents in Medicinal Chemistry, 22, (11), 2156–2165, 2022. https://doi.org/10.2174/1871520621666211115113226

[26] A. Shivashankarappa and K. R. Sanjay, *Escherichia coli*-based synthesis of cadmium sulfide nanoparticles, characterization, antimicrobial and cytotoxicity studies, Brazilian Journal of Microbiology, 51, (3), 939–948, 2020. https://doi.org/10.1007/s42770-020-00238-9

[27] Y. Yeni, H. Nadaroglu, M. S. Ertugrul, A. Hacimuftuoglu, A. Alayli, Antiproliferative effects of cadmium sulfide nanoparticles obtained from walnut shells by green synthesis method on SH-SY5Y cell line, Toxicology Reports, 13, 101818, 2024. https://doi.org/10.1016/j.toxrep.2024.101818

[28] S. Akhtar, S. Rehman, S. M. Asiri, F. A. Khan, U. Baig, A. S. Hakeem, M. A. Gondal, Evaluation of bioactivities of zinc oxide, cadmium sulfide and cadmium sulfide loaded zinc oxide nanostructured materials prepared by nanosecond pulsed laser, Materials Science and Engineering: C, 116, 111156, 2020. https://doi.org/10.1016/j.msec.2020.111156

[29] A. S. Bhadwal, R. M. Tripathi, R. K. Gupta, N. Kumar, R. P. Singh, A. Shrivastav, Biogenic synthesis and photocatalytic activity of CdS nanoparticles, Rsc

Advances, 4, (19), 9484–9490, 2014. https://doi.org/10.1039/C3RA46221H

[30] S. Munyai, Z. N. Tetana, M. M. Mathipa, B. Ntsendwana, N. C. Hintsho-Mbita, Green synthesis of Cadmium Sulphide nanoparticles for the photodegradation of Malachite green dye, Sulfisoxazole and removal of bacteria, Optik, 247, 2021. https://doi.org/10.1016/j.ijleo.2021.167851

[31] S. Aggarwal, Photooxidation of 2-Butanol by using CdS semiconductor nano-particles, International Journal of Applied Research, 2, 202–204, 2016.

[32] A. Hasani, H. Sharifi Dehsari, A. Amiri Zarandi, A. Salehi, F. A. Taromi, H. Kazeroni, Visible Light-Assisted Photoreduction of Graphene Oxide Using CdS Nanoparticles and Gas Sensing Properties, Journal of Nanomaterials, 2015, (1), 930306, 2015. https://doi.org/10.1155/2015/930306

[33] A. Hernández-Gordillo, P. Acevedo-Peña, M. Bizarro, S. E. Rodil, R. Gómez, Photoreduction of 4-Nitrophenol in the presence of carboxylic acid using CdS nanofibers, Journal of Materials Science: Materials in Electronics, 29, (9), 7345–7355, 2018. https://doi.org/10.1007/s10854-018-8724-x

[34] R. Sokary, H. A. Raslan, R. M. Fathy, Green synthesis of CdS/flaxseed mucilage nanocomposite films using gamma irradiation for packaging applications, Radiochimica Acta, 112, (6), 427–444, 2024. https://doi.org/10.1515/ract-2023-0251

[35] P. Patra, R. Kumar, C. Kumar, P. K. Mahato, Ni-incorporated cadmium sulphide quantum dots for solar cell: an evolution to microstructural and linear-nonlinear optical properties, Journal of Crystal Growth, 2022. https://doi.org/10.1016/j.jcrysgro.2022.126 542

[36] A. K. Verma, P. Chandra, A. Srivastava, R. K. Shukla, Optoelectronic studies of commercially and lab prepared cadmium sulfide chalcogenide, Research & Reviews: Journal of Material Sciences, 5, (2), 28–34, 2017. https://doi.org/ 10.4172/2321-6212.1000167

[37] H. I. Elhenawy, N. A. Toto, A. S. Eltaweil, H. K. Hussein, M. Augustyniak, L.M. El-Samad, Assessing the toxicity of green *Agaricus bisporus*-based cadmium sulfide nanoparticles on *Musca domestica* as a biological model. Scientific Reports, 14, 21519, 2024. https://doi.org/10.1038/s41598-024-70060-y

[38] V. Veeramani, H. Tamilselvan, M. Ramesh, J. M. Sasikumar, P. Prema, A. Barathinivas, K. R. Kumar, M. Hussain, C. R. Multisanti, C. Faggio, P. Balaji, In vivo assessment of the effects of zinc-doped cadmium sulphide nanoparticles synthesized using *Hypsizygus ulmarius* mushroom extract on paclobutrazol toxicity in zebrafish (*Danio rerio*) early-life stages. Environmental Pollution, 384, 127026, 2025. https://doi.org/10.1016/j.envpol.2025.127026

[39] S. Faisal, N. Akhtar, H. Ullah, M. Akif, I. Khan, F. Ali, N. Z. K. Mohmand, Antifungal and antibacterial activity of *Lathyrus aphaca* L. mediated green synthesized CdS nanoparticles and their characterization. Green Chemical Technology, 2(2), 10007, 2025. https://doi.org/10.70322/gct.2025.10007

[40] M. Jameel, M. A. Rauf, M. T. Khan, M. K. Farooqi, M. A. Alam, F. Mashkoor, M. Shoeb, C. Jeong, Ingestion and effects of green synthesized cadmium sulphide nanoparticles on *Spodoptera litura* as an insecticidal agent and their antimicrobial and anticancer activities. Pesticide Biochemistry and Physiology, 190, 105332, 2023. https://doi.org/10.1016/j.pestbp.2022.105332

[41] M. S. Alsaggaf, A. F. Elbaz, S. El Badawy, S. H. Moussa, Anticancer and antibacterial activity of cadmium sulfide nanoparticles by *Aspergillus niger*. Advances in Polymer Technology, 1–13, 2020. https://doi.org/10.1155/2020/4909054

[42] Z. Gholami, M. Dadmehr, N. B. Jelodar, M. Hosseini, F. Oroojalian, A. Pakdin Parizi, One-pot biosynthesis of CdS quantum dots through in vitro regeneration of hairy roots of *Rhaphanus sativus* L. and their apoptosis effect on MCF-7 and AGS cancerous human cell lines. Materials Research Express, 7, 015056, 2020. https://doi.org/10.1088/2053-1591/ab66ea

[43] S. C. Tudu, M. J. Zubko, J. Kusz, A. Bhattacharjee, CdS nanoparticles (<5 nm) green synthesized using *Termitomyces heimii* mushroom: structural, optical and morphological studies. Applied Physics A: Materials Science and Processing, 127, 1–9, 2021. https://doi.org/10.1007/s00339-020-04245-3

[44] S. R. Pandian, V. Deepak, K. Kalishwaralal, S. Gurunathan, Biologically synthesized fluorescent CdS nanoparticles encapsulated by PHB. Enzyme and Microbial Technology, 48(4–5), 319–325, 2011. https://doi.org/10.1016/j.enzmictec.2011.01.005

[45] R. Sanghi and P. Verma, A facile green extracellular biosynthesis of CdS nanoparticles by immobilized fungus, Chemical Engineering Journal, 155, (3), 886–891, 2009. https://doi.org/10.1016/j.cej.2009.08.006

[46] R. Lakshmipathy, N. C. Sarada, K. Chidambaram, S. Pasha, One-step, low-temperature fabrication of CdS quantum dots by watermelon rind: a green approach. International Journal of Nanomedicine, 10(Supplement 1), 183–188, 2015. https://doi.org/10.2147/IJN.S79988

[47] G. T. Elakkiya, G. Sundararajan, R. Lakshmipathy, P. Anitha, N. Muruganantham, Prolific application of green synthesised CdS nanoparticles for the sequestration of cationic dyes from aqueous solution. Bulletin of the Chemical Society of Ethiopia, 38(3), 631–645, 2024. https://doi.org/10.4314/bcse.v38i3.7

[48] K. Prasad and A. K. Jha, Biosynthesis of CdS nanoparticles: an improved green and rapid procedure. Journal of Colloid and Interface Science, 342(1), 68–72, 2010. https://doi.org/10.1016/j.jcis.2009.10.003

[49] H. Bai, Z. Zhang, Y. Guo, W. Jia, Biological synthesis of size-controlled cadmium sulfide nanoparticles using immobilized *Rhodobacter sphaeroides*. Nanoscale Research Letters, 4, 717, 2009. https://doi.org/10.1007/s11671-009-9303-0

[50] M. Borovaya, Y. Pirko, T. Krupodorova, A. Naumenko, Y. Blume, A. Yemets, Biosynthesis of cadmium sulphide quantum dots by using *Pleurotus ostreatus* (Jacq.) P. Kumm. Biotechnology and

Biotechnological Equipment, 1–8, 2015. https://doi.org/10.1080/13102818.2015.1064264
[51] J. Falandysz, T. Kunito, R. Kubota, M. Gucia, A. Mazur, J. J. Falandysz, S. Tanabe, Some mineral constituents of parasol mushroom (*Macrolepiota procera*). Journal of Environmental Science and Health, Part B, 43(2), 187–192, 2008. https://doi.org/10.1080/03601230701795247
[52] I. Adamska and G. Tokarczyk, Possibilities of Using *Macrolepiota procera* in the Production of Prohealth Food and in Medicine, International Journal of Food Science, 2022, 1–27, 2022. https://doi.org/10.1155/2022/5773275
[53] M. Kosanić, B. Ranković, A. Rančić, T. Stanojković, Evaluation of metal concentration and antioxidant, antimicrobial, and anticancer potentials of two edible mushrooms *Lactarius deliciosus* and *Macrolepiota procera*. Journal of Food and Drug Analysis, 24(3), 477–484, 2016. https://doi.org/10.1016/j.jfda.2016.01.008
[54] J. Sabotič, S. Kilaru, M. Budič, M. B. Gašparič, K. Gruden, A. M. Bailey, G. D. Foster, J. Kos, Protease inhibitors clitocypin and macrocypin are differentially expressed within basidiomycete fruiting bodies. Biochimie, 93(10), 1685–1693, 2011. https://doi.org/10.1016/j.biochi.2011.05.034
[55] A. Kalia and G. Kaur, Biosynthesis of nanoparticles using mushrooms. Biology of Macrofungi, 351–360, 2018. https://doi.org/10.1007/978-3-030-02622-6_17
[56] M. S. Sadjadi and A. Khalilzadegan, The effect of capping agents, EDTA and Eg on the structure and morphology of CdS nanoparticles, Journal of Non-Oxide Glasses, 7, (4), 55–63, 2015.
[57] V. Singh and P. Chauhan, Synthesis and structural properties of wurtzite type CdS nanoparticles, Chalcogenide Letters, 6, (8), 421–426, 2009.
[58] M. S. Geetha, H. Nagabhushana, H. N. Shivananjaiah, Green mediated synthesis of Ce-doped CdO nanocrystals: study of its magnetic and photoluminescence characteristics, Materials Science, 3, 2456–3293, 2018.
[59] D. Ayodhya, M. Venkatesham, A. Santoshi Kumari, G. Bhagavanth Reddy, G. Veerabhadram, One-pot sonochemical synthesis of CdS nanoparticles: photocatalytic and electrical properties, International Journal of Industrial Chemistry, 6, (4), 261–271, 2015. https://doi.org/10.1007/s40090-015-0047-7
[60] H. K. Yagmur, I. Kaya, H. Aydin, Synthesis, characterization, thermal and electrochemical features of poly(phenoxy-imine)s containing pyridine and pyrimidine units. Journal of Polymer Research, 27(12), 356, 2020. https://doi.org/10.1007/s10965-020-02297-w
[61] L. E. Brus, Electron–electron and electron–hole interactions in small semiconductor crystallites: the size dependence of the lowest excited electronic state. The Journal of Chemical Physics, 80(9), 4403–4409, 1984. https://doi.org/10.1063/1.447218
[62] L. Spanhel, M. Haase, H. Weller, A. Henglein, Photochemistry of colloidal semiconductors. 20. Surface modification and stability of strong luminescing CdS particles, Journal of the American Chemical Society, 109, (19), 5649–5655, 1987. https://doi.org/10.1021/ja00253a015
[63] W. W. Yu, L. Qu, W. Guo, X. Peng, Experimental Determination of the Extinction Coefficient of CdTe, CdSe, and CdS Nanocrystals, Chemistry of Materials, 15, (14), 2854–2860, 2003. https://doi.org/10.1021/cm034081k
[64] M. J. Lim, N. N. M. Shahri, H. Taha, A. H. Mahadi, E. Kusrini, J. W. Lim, A. Usman, Biocompatible chitin-encapsulated CdS quantum dots: fabrication and antibacterial screening. Carbohydrate Polymers, 260, 117806, 2021. https://doi.org/10.1016/j.carbpol.2021.117806
[65] S. Basak and R. Das, Optical properties of synthesized hexagonal CdTe nanoparticles with hexagonal phase: density functional theory-supported calculation of band gap and density of states, Physica Status Solidi (B), 260, (1), 2200157, 2023. https://doi.org/10.1002/pssb.202200157
[66] U. S. Senapati and D. Sarkar, Characterization of biosynthesized zinc sulphide nanoparticles using edible mushroom *Pleurotuss ostreatu*, Indian Journal of Physics, 88, (6), 557–562, 2014. https://doi.org/10.1007/s12648-014-0456-z
[67] C. Baudot, C. M. Tan, J. C. Kong, FTIR spectroscopy as a tool for nano-material characterization, Infrared Physics & Technology, 53, (6), 434–438, 2010. https://doi.org/10.1016/j.infrared.2010.09.002
[68] C. Dias, M. Ayyanar, S. Amalraj, P. Khanal, V. Subramaniyan, S. Das, P. Gandhale, V. Biswa, R. Ali, N. Gurav, Biogenic synthesis of zinc oxide nanoparticles using mushroom fungus *Cordyceps militaris*: characterization and mechanistic insights of therapeutic investigation. Journal of Drug Delivery Science and Technology, 73, 103444, 2022. https://doi.org/10.1016/j.jddst.2022.103444
[69] A. Parihar, P. Sharma, N. K. Choudhary, R. Khan, A. Gupta, R. K. Sen, H. C. Prasad, M. Ashiq, Green Synthesis of CdS and CdS/rGO Nanocomposites: Evaluation of Electrochemical, Antimicrobial, and Photocatalytic Properties, ACS Applied Bio Materials, 6, (9), 3706–3716, 2023. https://doi.org/10.1021/acsabm.3c00390
[70] C. K. Sheng and Y. M. Alrababah, pH-induced wurtzite-zinc blende heterogeneous phase formation, optical properties tuning and thermal stability improvement of green synthesized CdS nanoparticles, Heliyon, 9, (5), 2023. https://doi.org/10.1016/j.heliyon.2023.e15908
[71] A. Elfalaky, A. F. Mansur, F. A. Maged, Polyaniline–CdS nanocomposite: synthesis, structural, thermal and spectroscopic analysis. IOSR Journal of Applied Physics, 7(3), 92–100, 2015.
[72] I. H. Hadi, K. S. Khashan, D. Sulaiman, Cadmium sulphide (CdS) nanoparticles: preparation and

characterization, Materials Today: Proceedings, 42, 3054–3056, 2021. https://doi.org/10.1016/j.matpr.2020.12.828

[73] K. Manikandan, C. S. Dilip, P. Mani, J. J. Prince, Deposition and characterization of CdS nano thin film with the complexing agent triethanolamine, American Journal of Engineering and Applied Sciences, 8, (3), 318–327, 2015. https://doi.org/10.3844/ajeassp.2015.318.327

[74] A. Regmi, Y. Basnet, S. Bhattarai, S. K. Gautam, Cadmium Sulfide Nanoparticles: Synthesis, Characterization, and Antimicrobial Study, Journal of Nanomaterials, 2023, 1–7, 2023. https://doi.org/10.1155/2023/8187000

[75] S. R. Sam, S. L. Rayar, P. Selvarajan, Effect of annealing and dopants on the physical properties of CdS nanoparticles. Journal of Chemical and Pharmaceutical Research, 7(3), 957–963, 2015.

[76] N. Soltani, E. Gharibshahi, E. Saion, Band gap of cubic and hexagonal CdS quantum dots: experimental and theoretical studies. Chalcogenide Letters, 9(7), 321–328, 2012.

[77] P. Scherrer, Estimation of the size and internal structure of colloidal particles by means of Röntgen. Nachrichten von der Gesellschaft der Wissenschaften zu Göttingen, Mathematisch-Physikalische Klasse, 2, 96–100, 1918.

[78] A. Singer, Z. Barakat, S. Mohapatra, S. S. Mohapatra, Nanoscale drug-delivery systems: in vitro and in vivo characterization, Nanocarriers for drug delivery, 395–419, 2019. https://doi.org/10.1016/B978-0-12-814033-8.00013-8

[79] J. Jiang, G. Oberdörster, P. Biswas, Characterization of size, surface charge, and agglomeration state of nanoparticle dispersions for toxicological studies, Journal of Nanoparticle Research, 11, (1), 77–89, 2009. https://doi.org/10.1007/s11051-008-9446-4